IEEE Access
Multidisciplinary | Rapid Review | Open Access Journal

Received September 4, 2018, accepted September 26, 2018, date of publication October 10, 2018,
date of current version November 8, 2018.

Digital Object Identifier 10.1109/ACCESS.2018.2875071

A Review of Turbidity Detection Based on Computer Vision

YEQI LIU, YINGYI CHEN, AND XIAOMIN FANG
College of Information and Electrical Engineering, China Agricultural University, Beijing 100083, China
Key Laboratory of Agricultural Information Acquisition Technology, Ministry of Agriculture, Beijing 100083, China
Beijing Engineering and Technology Research Center for Internet of Things in Agriculture, Beijing 100083, China

Corresponding author: Yingyi Chen (chenyingyi@cau.edu.cn)

This work was supported in part by the Shandong Province Key Research and Development Program called Research and Demonstration of Accurate Monitoring and Controlling Technologies for Environment of Vegetable in Facility under Grant 2017CXGC0201 and in part by the Science and Technology Program of Beijing called Research and Demonstration of Technologies Equipment Capable of Intelligent Control for Large-Scale Healthy Cultivation of Freshwater Fish under Grant Z171100001517016.

ABSTRACT Computer vision technology has made great progress in practice in recent years, and it also has broad application prospects in turbidity detection. Turbidity detection plays an important role in water environment science, but popular turbidity detection methods have some limitations in aspects of cost, convenience, and space-time coverage. Based on above reasons, researchers are devoted to developing image-based turbidity detection methods as a complementary or even alternative to the popular turbidity detection method. However, the use of computer vision technology to detect turbidity is affected by many factors such as imaging system, feature extraction, model selection, and so on. Currently, there is no comparison and analysis of these methods in a framework. Therefore, this paper introduces typical turbidity detection methods based on computer vision in detail, with their principle, measurement range, accuracy, technical framework, and comparison. In this paper, existing studies are divided into four types according to different image sources, and seven image features mainly used in these studies are pointed out. The objective of this paper is to review the development status, existing problems, future research directions of image-based turbidity detection methods, and establishment of a unified framework which includes principles, technical framework, and main equipment of imaging systems.

INDEX TERMS Computer vision, turbidity detection, feature extraction, imaging system, water quality, application.

I. INTRODUCTION

Water is the source of mankind and all lives. Turbidity, which refers to a common usage of the term that is the optical clarity of water or liquid, is an important indicator of water quality detection. Turbidity is also a relative indicator used to replace other physical properties such as suspended sediment concentration (SSC) and total suspended solids (TSS) [1], [2]. In addition, turbidity can reflect the content of other substances in the water, such as chlorophyll, organic matter, microorganisms, etc. [3], [4]. Hence, turbidity detection is of great significance for environmental protection, aquatic ecosystems, and drinking water safety [5]–[7].

At present, turbidimeter is a widely used turbidity detection method, which includes laboratory detection methods and online instrument detection methods. The advantage of laboratory detection methods is high accuracy [8]. However, there are some obvious disadvantages, e.g., high cost, professional operation, lack of real-time performance, and impossible to obtain accurate samples in large spaces and long-time spans. On the contrary, online instrument detection methods are guaranteed in real-time, but its accuracy is easily affected by stains in water. It is also difficult to be fixed and be cleaned in the center of water [9], and high cost of instrument deployment makes it difficult to undertake. Meanwhile, the difficulty to operate and fragile instrument features are also huge challenges for its use and promotion.

With the development of computer vision, it has become one of the most successful fields of artificial intelligence at present, and many related technologies have been developed rapidly and industrialized, such as face recognition [10], autonomous vehicles [11], and plant identification [12]. Additionally, this technology has been applied to water

quality monitoring, such as the detection of chlorophyll and flocculating agent [13], [14]. Turbidity detection based on computer vision is not only beneficial to water environment research and protection, but also plays an important role in underwater machine vision and environmental awareness of citizen [15], [16]. Using computer vision, we can get high-resolution images and accelerate the model establishment through cheap but parallel hardware, extract more salient features and achieve better image interpretation through state-of-the-art algorithms, and build a model with good generalization and high accuracy through big data in the Internet of Things.

Therefore, computer vision technology provides enough theoretical and practice basis for turbidity detection. This technology with low-cost, high-precision, simple to operation, and easy to promote features can arrive at a good level with economic and social benefits. The main factors that have led to the development of turbidity detection methods based on computer vision are: (1) it benefits from the development of computer vision and pattern recognition, e.g., algorithm, hardware, and image data; (2) the prospect of achieving high accuracy and high resolution is proven in existing researches; (3) it provides a kind of turbidity detection method to balance cost, convenience, and space-time coverage; (4) it is of great significance to the awareness of water environment protection for each citizen. For example, the use of smartphones is suitable for environmentalists and even each citizen to supervise water quality; the use of surveillance video is suitable for long-term water quality observations; and the use of UAVs (unmanned aerial vehicles) for shooting is suitable in larger areas.

In this paper, we introduce the principle, method, and system of turbidity detection methods based on computer vision technology in detail. First of all, it is found that image-based turbidity detection methods have wide application value by comparing with the current popular turbidity detection methods. Secondly, we sum up a unified framework of principles, technical framework, and main equipment of imaging systems. Thirdly, we summarize four types of methods according to different image sources including sampled image, underwater image, water surface image, and invisible light image. The classification criteria are based on differences in image acquisition methods and differences in image features. Note, the invisible light image, such as infrared image and remote sensing image, has been widely used in turbidity monitoring of the river basin [17], [18]. In the first three types of methods, we review seven image features. Finally, we compare the range and accuracy of these methods from three perspectives with typical methods, image sources, and image features.

This paper helps to find a turbidity detection method used in a wider range of applications to replace the fragile, expensive, difficult to maintain and operate instrument detection method. This review will attract more researchers in the field of computer vision to develop image-based turbidity detection technology. In particular, the application of this technology to smartphones will enhance the protection of the water environment and aquatic ecosystems by governments and citizens. Additionally, this paper also provides ideas for the detection of other water quality parameters, e.g., chlorophyll detection, which will help develop a new water quality detection technology. In conclusion, we provide a comparison and framework to find better feature extraction and modeling methods, and we also present state-of-the-art turbidity detection methods based on computer vision, which balance cost, convenience, and space-time coverage. The framework and summary of existing literatures are shown in Fig. 1, with more details presented in Section 2 and Section 3. The main contributions of this review article are as follows:

- Four types of methods are divided according to the different sources of image acquisition.
- Seven kinds of image features are summarized based on different image features.
- A unified framework has been established which includes principles, technical framework and typical systems.
- The quantitative comparison of the range and error of the existing methods.
- The future work is directed such as systems, algorithms and unified standards.

The rest of paper is organized as follows. Section 2 presents some basic concepts of turbidity and the comparison of popular turbidity detection methods. In addition, it also summarizes a unified principle, system, and technical framework. Section 3 reviews the existing research from four types and seven image features, and summarizes the characteristics and improvements of each type. In Section 4, we discuss the feasibility of using computer vision technology to detect turbidity through quantitative analysis. Finally, we give a conclusion for the paper, and point out some potential improvement in future.

II. FRAMEWORK OF TURBIDITY DETECTION BASED ON COMPUTER VISION

In this section, we first introduce some basic concepts related to this paper, e.g. turbidity units and mainstream measurement methods, and then compare the mainstream turbidity detection methods and image-based turbidity detection methods. Next, basic principle of image-based turbidity detection method is introduced, and system structures and technical framework are summarized. Finally, turbidity detection methods based on computer vision are classified into four types according to different sources of images.

A. CONCEPTS AND CONTRASTS

The widely used turbidity units are FNU, NTU, FTU, and FAU. In Table 1, we present measurement principles of these units, standard solutions required, standard organization, and instruments that use these units. In conclusion, only FAU is measured by spectrophotometer [19]. The principle corresponding to different units is generally different, and turbidity units in the references are not uniform, but they are all calibrated by Formazin solution, so these units are equal

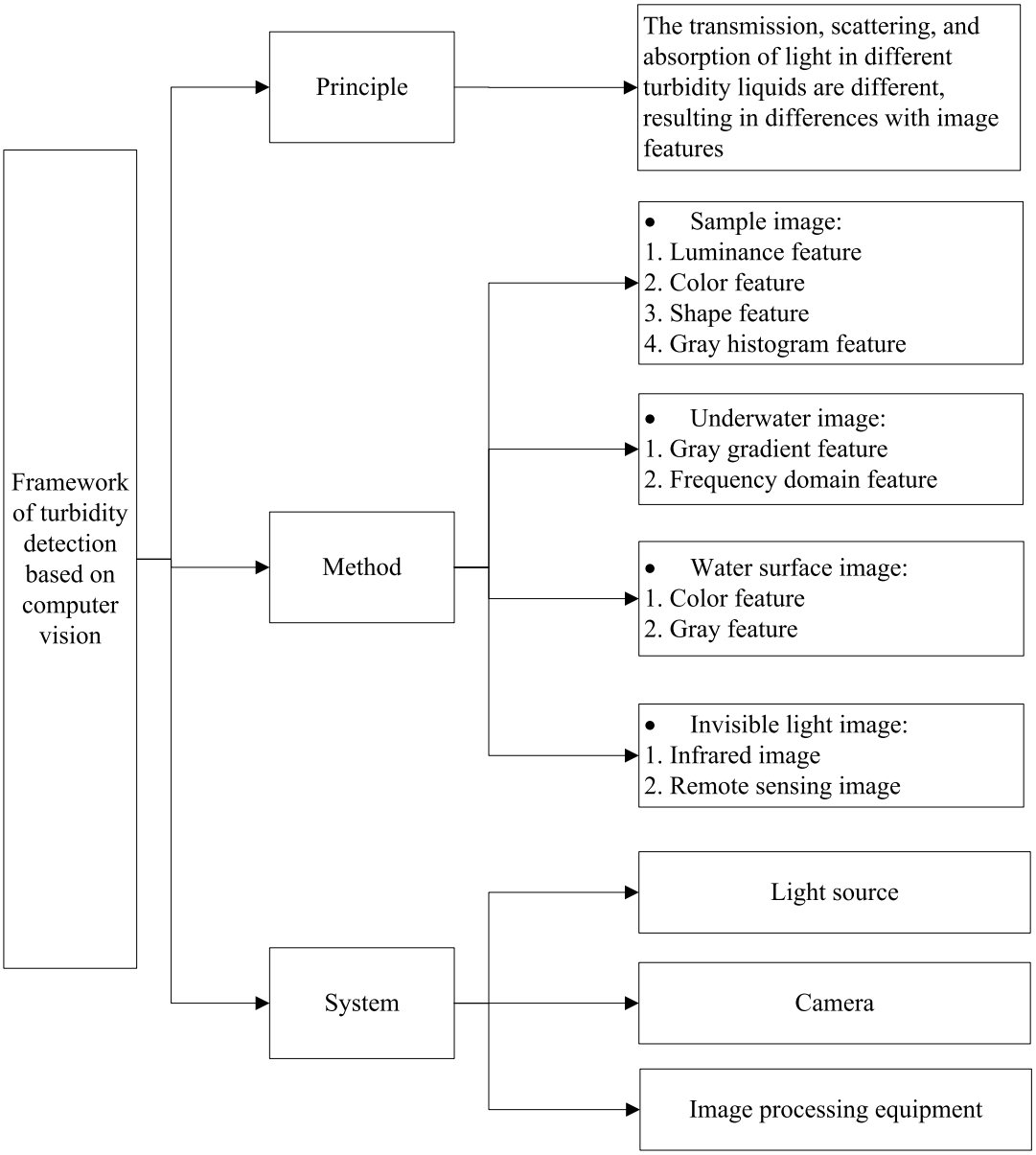

FIGURE 1. Framework of turbidity detection based on computer vision.

in measuring turbidity with the same standard solution [20]. In this paper, NTU is used as turbidity unit and converts all other units used in the reference.

The turbidimeter is the main method to measure turbidity at present. As shown in HASH 2100AN turbidimeter [21], the measurement range is 0-10000 NTU, the error is distributed between 2% and 10% according to different range settings, and the resolution can reach 0.001 NTU. However, the price of this instrument can be as high as thousands of dollars. In contrast, the spectrophotometer has a low cost for the turbidimeter, but it only uses the attenuation degree of the transmitted light as the measurement principle, resulting in a large error in the measurement result [22]. The earlier measurement method is visual nephelometry, and the principle of this method is to observe the similarity between sample and standard solution by human eyes [23]. In Table 2, we compare these methods to show that the image-based method has good balance between cost, accuracy, and convenience.

B. PRINCIPLES AND METHODS

Compared with visual nephelometry method and instrumental analysis method, the turbidity detection method based on computer vision can be applied to more scenes because of different image acquisition methods. According to different sources of images, we classify the turbidity detection methods based on computer vision into four types: sampled image, underwater image, water surface image, and invisible light image.

TABLE 1. Different turbidity units (the use of NTU in the review article).

Unit	Abbreviation	Principle	Standard solution	Standard Organization	Instrument
Formazin Nephelometric Unit	FNU	light scattering	Formazin	International Organization for Standardization (ISO)	Turbidimeter
Nephelometric Turbidity Unit	NTU	light scattering	Formazin	U.S. Environmental Protection Agency (USEPA)	Turbidimeter
Formazin Turbidity Unit	FTU	light scattering	Formazin	American Public Health Association (APHA)	Turbidimeter
Formazin Attenuation Unit	FAU	light transmission	Formazin	International Organization for Standardization (ISO)	Spectrophotometer

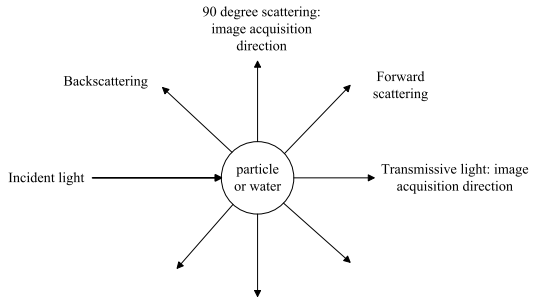

FIGURE 2. The principle of turbidity detection methods based on computer vision.

In general, the basic principle of these methods is same, which is summarized in Fig. 2. When light source is irradiated into the liquid, because the absorption, transmission, and scattering of the light in the liquid with different turbidity level are different, and the degree of attenuation is measured in different ways (e.g. photoelectric converter, imaging, etc.) from different angles. Moreover, the relationship model between turbidity values and image features is established. As shown in Fig. 2, when light passes through impurity particles in water, attenuation will occur in all directions [2]. When the measured liquid is regarded as a whole, whether using a turbidimeter or computer vision methods, the attenuation degree in the transmission direction, the 90 degree scattering direction, or both directions can be measured. Therefore, the idea of image-based turbidity detection method still does not deviate from the popular methods. Whether using turbidimeter or image-based methods, the basic principle are both attenuation degrees of absorption, transmission, or scattering when the light passes through different turbidity liquid. These methods basically all require standard comparison or standard proofreading established by instruments such as turbidimeter. According to this principle, the basic structure of turbidity detection system based on computer vision includes light source, image acquisition device, and image processing equipment.

As shown in Fig. 3, it is one of the key steps to establish the correspondence between image features and standard comparison libraries in the technical framework, which is similar to image annotation in the field of computer vision. The entire technical framework is mainly composed of five modules: water image acquisition, image preprocessing, feature extraction, establishment of a standard comparison library, and determination of correspondence relationship. No matter the interference of light, background, and even imaging technology, all images contain some noise, so the preprocessing of the image, such as image denoising, image enhancement, image segmentation, etc., is not necessary, but it is effective to improve accuracy.

Nevertheless, there are also some differences of how to preprocess images from different sources. For example, it is not necessary to enhance images if high-contrast background is artificially set for sampling. In feature extraction module, this paper presents seven image features, including luminance, color, shape, gray histogram, frequency domain feature, gray feature, and gray gradient. The establishment of a precise standard comparison library is important to ensure accuracy. In the establishment of relational model, we can establish linear relationship, polynomial relationship, power relationship, and neural network model between extracted features and standard comparison libraries. In addition, the standard comparison library is used to obtain the turbidity value of the water to be measured by turbidimeter, or to obtain the corresponding image of the water to be measured with equal turbidity interval in the turbidity measurement range. Finally, we establish a turbidity discriminant model through the standard comparison library, that is, the model between the image features and measured values, or the model between the water image to be measured and the reference turbidity image in the standard comparison library, so as to obtain the corresponding turbidity value of the real-time image.

Turbidity detection is performed based on images from different sources, and different image sources correspond to different application scenarios. Based on this reason, we set

TABLE 2. Comparison between popular methods and the image-based method.

Method	Precision (%)	Range (NTU)	Applicable fields	Principle	Advantage	Disadvantage
Visual nephelometry	>10 [23]	>1, and low range	Turbidity estimation	Comparison of water samples and standard samples with human eyes.	1. operation is simple 2. fast measurement speed	1. visual acuity, experience, and other human factors have great influence on measurement. 2. low accuracy and poor reproducibility.
Spectrophotometer	>5 (Macy Instrument)	1-1000	Multi-parameter measurement	Light transmission based on Lambert-Beer Law [24].	1. balance between cost and precision 2. instrument versatility	1. lower accuracy than turbidimeter, because only using transmission light can not accurately reflect the attenuation degree of light.
Turbidimeter	2-10 [21]	0 -10000	High precision measurement	The method can be classified into transmission method, scattering method, and the ratio method between scattering and transmission light.	1. high resolution 2. high accuracy	1. high cost. 2. artificial sampling or fixed instruments are not suitable for sampling in large space and long time.
Turbidity detection methods based computer vision	>2.8 [25]	0-6000	Different image acquisition methods lead to multipurpose	The model is established based on the relationship between image features and standard comparison library.	1. different image acquisition methods are suitable for different application scenarios. 2. balance between cost, convenience, and space-time coverage.	1. accuracy is slightly lower than the instrumental analysis method, so it is limited for high-precision measurement so far.

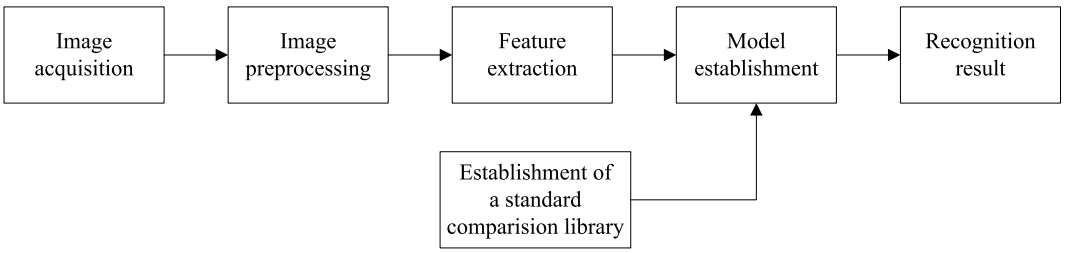

FIGURE 3. The technical framework of turbidity detection methods based on computer vision.

up a classification standard for image-based turbidity detection methods. These methods are not applicable to the same range of time and space. Turbidity detection methods based on the sampled image do not have advantages in time, space, and cost, because sampling is artificially needed, but it can improve the accuracy because it is under a controllable sampling condition such as manual control of the background and light source. Turbidity detection methods based on underwater image have no spatial advantage, but it can be adapted to long-term and fixed-point detection in the underwater vertical delamination. Turbidity detection methods based on water surface images can be applied to different occasions because the direct shooting methods can also be different, e.g. smartphone, surveillance, aerial photography, etc. Turbidity detection methods based on remote sensing image can be applied to long-term and whole-basin turbidity detection.

III. TURBIDITY DETECTION WITH DIFFERENT IMAGE SOURCES

In this section, there are four types of turbidity detection methods based on computer vision from different image sources. The general idea of each method is the same, that is,

to establish a relationship model between acquired images and standard comparison libraries. However, different image sources lead to different system structures, different image processing methods, and different relationship models. The details of typical turbidity detection methods based on computer vision are summarized in Appendix. For each method, we introduce principles, main system structures, and technical framework according to the unified technical framework.

A. SAMPLED IMAGE

The turbidity detection method based on sampled images is artificially sampled, and then water sample is placed in a specific environment for image acquisition. Next, the extracted features are compared to a standard comparison library to establish a relationship between turbidity value and image features.

1) LUMINANCE

The degree of attenuation from the luminance of different sample images can reflect the turbidity value in a sample. Mullins *et al.* [26] proposed a turbidity detection method based on sampled images called camera estimated turbidity (CET). As shown in Fig. 4(a), the whole system consists of glass vessel, infrared light source, and complementary metal oxide semiconductor (CMOS) camera, which is a typical system structure of sampled image methods. Moreover, stirrer is also used in the CET method to keep a uniform turbidity distribution of sample, but it is not drawn in the vessel for simplicity and uniformity. In CET, the camera shutter is controlled by MATLAB program, which can obtain multiple images of each sample, and then the average value of light intensity is used to reduce error. The direction of light source is orthogonal to the direction of camera, similar to the 90 degree scattering principle of the instrument measurement method.

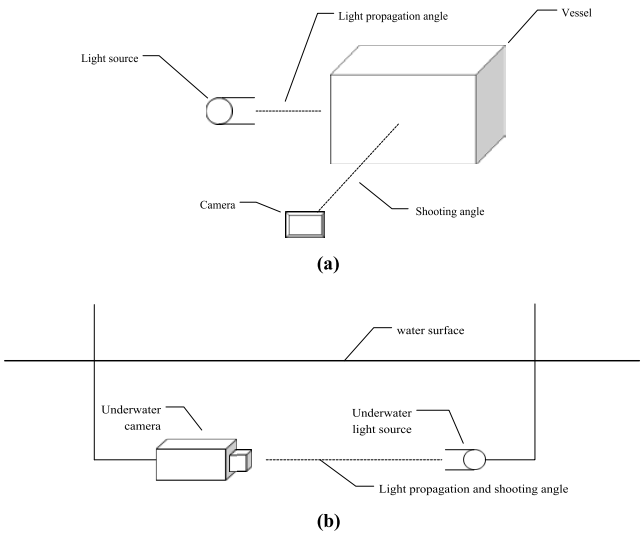

FIGURE 4. Typical systems of turbidity detection methods based on computer vision. (a) Typical systems based on sampled image. (b) Typical systems based on underwater image.

The design idea of CET method is roughly the same as most turbidity detection methods based on computer vision, which can be divided into image acquisition, image preprocessing, feature extraction, establishment of a standard comparison library, and establishment of a corresponding relationship between standard libraries and image features. The image preprocessing module mainly includes image segmentation. Before this operation, the sample image is augmented by mixing and diluting samples with different ratios to obtain a larger image dataset. Image segmentation is to avoid the impact of vessel structure on experiments, and the vortex area should be separated when the sample is stirred by agitators. This method selects 3/11 part in the middle of the vessel as a region of interest (ROI), which is the width of measurement channel for measuring the attenuation degree of light. The extracted image feature is the number of pixels in the ROI when the incident light intensity drops to 63% of the intensity of light source. The standard comparison library is established by using spectrophotometer to measure the average value of water samples correspondingly. The corresponding relationship is a linear relationship between the numbers of pixels whose luminance is higher than the threshold and the measured turbidity value.

2) COLOR

It may be a very intuitive method to establish the model between color features and turbidity, but color features are decomposed into combination of red, blue, and green band (RGB). Hamidi *et al.* [27] used smartphones to acquire RGB images, and then convert them to mean greyscale index (MGI). Moreover, the regression relationship between MGI and standard turbidity sample is established. However, the measurement rang of this method is only 0 to 100 NTU. Toivanen *et al.* [28] and Näykki *et al.* [29] described a device called Secchi3300. The system contains Secchi3300 measurement device, smartphone with a measurement application (MA), and a server for image processing and standard library storage. In order to get the maximum luminance, the plastic container (i.e., vessel) of Secchi3300 is transparent on one side that needs to face the brightest part of the sky. There are white, black, and gray object regions in two parts of the plastic container at two vertical intervals. MA is used to send pictures, addresses, and time information to the server. The role of the server includes receiving images, extracting features, determining, and result feedback.

The principle of Secchi3000 method is based on comparison of light intensity measured over black, white, and grey object regions at two depths. The design idea of this device is originated from Seccci Disk (SD) [30], and the technical framework of Secchi3300 can also be divided into five modules from the general idea of image-based turbidity detection methods. The way of image acquisition is to capture images through a small hole on the container, and further process includes template matching and image segmentation. The extracted feature is reflectivity difference of the same color area at different depths. Meanwhile, the establishment

of standard comparison library is based on laboratory instruments to detect the same samples correspondingly, and linear relationship model is established and also calibrated by laboratory measurements such as turbidimeter.

However, the Secchi3000 method can only detect one sample at a time. Wang *et al.* [25] proposed a more automated method that detects turbidity based on RGB reflectivity of sampled images. The main equipment of their system includes charge-coupled device (CCD) camera, light source, filter, card feeding system, and computer. The reason why the blue filter is chosen is that CCD crystal has high absorption of blue light on the surface of silicon crystal. A card feed system is used to automatically acquire different sample images. Later, image processing is done on the computer. The technical framework of this method is also divided into five modules, and the standard comparison library is still measured by a turbidimeter in laboratory. It is found that the changes in the B band have significant regularity in features of three RGB bands, but in order to avoid the influence of brightness and temperature, the difference value of B band and G band is used in the experiment as the final image feature. Finally, three degree polynomial is used as discriminant model. This method is more automated through card feed system, and CCD unit can acquire images from multiple samples automatically and quickly. This method is satisfactory in range and accuracy because of band combination and CCD camera selection. Pilz *et al.* [31] describes optical characteristics of CCD and light source composition systems, and indicated that there are more suitable light sources for this type of systems.

Jamale and Pardeshi [32] presented a turbidity detection method which is slightly different from the above method. The difference is that the standard comparison library is the RGB relationship between standard turbidity images and measured images, i.e., the image-to-image correspondence is directly used instead of the image-to-value correspondence. However, measurement range of this method is only 0-5 NTU, and accuracy is worse than that of CCD method. In contrast, the equipment of this method is relatively simple. The system consists of light source, camera, computer, and white container in a box. Firstly, samples are placed in the box to avoid interference from external light and other background. Secondly, standard turbidity samples between 0-5 NTU are configured. They photograph images of these samples, record their maximum and minimum values of RGB reflectivity as extracted features, and set up a standard comparison library including these feature values. Thirdly, maximum and minimum values of RGB reflectivity are compared and a nearest rank is found in the standard comparison library. This method is low in cost and helps to avoid background and light interference, but the measuring range is small. One of main reasons is that the relationship model between sample image and turbidity value is not directly established, but the feature relationship between sample images and standard image is established. Another reason is that this method uses only a sealed dark environment as the background.

3) SHAPE

In the method of detecting turbidity from image shape features, the shape features are manually set, and the relationship model is built by the number or quality of the target shape that can be detected in different turbidity samples. Robust shape detection algorithms, e.g., circles, lines, etc., are selected in computer vision. Chai *et al.* [33] proposed a method to detect the number of circles under different turbidity levels. The system is composed of camera, sampling container, light source, image processing unit, bracket, etc. Among them, the sample container with circular rings at the bottom, which can lift automatically, is the key for feature extraction, and the automatic elevator is used to find an appropriate imaging distance. Moreover, the circular rings are detected by circle detection algorithms in MATLAB algorithms library. Meanwhile, the principle of feature extraction is that the numbers of rings that can be detected under different turbidity levels are different, and the turbidity value of laboratory instruments is used to create a standard comparison library, and then the relationship model including linear function and logarithmic function between the standard comparison library and the number of rings is established. This system can be continuously measured by continuous pumping and drainage from water sample for measurement. In conclusion, the main difference between this method and the methods based other image features is the large requirement for image preprocessing and the high-accuracy requirement of pattern recognition algorithms for circular detection.

4) GRAY HISTOGRAM

The image grayscale feature is a statistical representation of grayscale distribution. As turbidity of the sample increases, the grayscale distribution deviates from the origin in the gray histogram. Karnawat and Patil [34] described a turbidity detection method based on image gray histogram. The system consists of camera, transparent container, light source, and computer. Similar to CET method, the position of the light source and camera are orthogonal. The technical framework of this method can be also divided into five modules, and the image preprocessing includes some general ways such as grayscale transformation, image filtering, and thresholding. In addition, the minimum resolution of these sample images is 620∗850, which is sure to extract enough salient features. This method describes that gray histogram is more distributed in the range of 120-180 grayscale value, and the extracted feature is the peak value in this range. Finally, the standard comparison library is to establish a corresponding table between laboratory measurement values and spiking values. One advantage of this method is that the method does not need to keep stirring to maintain turbidity evenly of water sample compared with above methods. Another advantage is that it does not even require a specific container, so it can be sampled and photographed with any transparent plastic bottle.

5) SUMMARY

The main factors affecting the accuracy of different feature extraction are different. For example, we pay more attention to RGB band combinations in color features, but we pay more attention to the detection algorithm selection in shape features. However, sampled image is under a controlled condition, which is a key factor for the higher accuracy of this method compared to other image acquisition methods, so we can improve the accuracy through the following improvements:

- Background, light source, and camera. For background selection in containers, stronger contrast background can be selected, so that the contrast with ROI is more obvious. For light source selection, the more appropriate light source which attenuates more slowly can be chosen, e.g., infrared light source is less easily attenuated. Meanwhile, the camera with higher photosensitivity and higher resolution can be used to get more salient details.
- Sampling method. Inspired by Effler *et al.* [35], we can use underwater robots to sample, so that we can get more accurate turbidity measurement plots in different vertical layers of water.
- Automation. Automatic sampling, automatic transmission, automatic cleaning and automatic fault detection are necessary for automation. For example, an integrated system can be constructed using CET method, in which a camera and a communication equipment are fixed in the system, and the container is added with automatic pumping and auxiliary equipment with cleaning function, so that images can be acquired and processed automatically, and the turbidity information of water quality can be obtained at a fixed location periodically.

B. UNDERWATER IMAGE

The turbidity detection method based on underwater images is very important for long-term and fixed-point detection, which can detect turbidity changes at different water depths. The special device of this method is that it needs a special underwater camera and underwater light source, which will increase its cost and operation difficulty. In addition, the uncertainty of the underwater background and the adhesion of impurities are also great challenges for this method.

1) GRADIENT AND FREQUENCY DOMAIN FEATURE

Underwater image acquisition generally only obtains the halo image of the light source in water, so the frequency domain features are more significant. Li [36] proposed a turbidity detection system based on underwater images. The system structure is shown in Fig. 4(b), which is composed of underwater light source, underwater camera, and image processing terminal. The camera collects images transmitted by the light source and connected to the image processing terminal, which can be divided into five modules: image preprocessing, feature extraction, standard library establishment, correspondence relationship establishment, and result discrimination.

The image obtained by the system is a halo image generated after the light source transmits through water, and the halo image features are different due to different turbidity. Firstly, gray gradient features in spatial domain and spectrum features in frequency domain are extracted. Moreover, a relationship model is trained by the back propagation (BP) neural network, and the turbidity detection is carried out by this BP model. The function of the image standard library is to add turbidity labels to the feature data and verify the correctness of BP model. Next, wavelet transform is used to extract spectrum features. There are 4 hidden layers in BP neural network structures, and each layer includes 10 neurons. The output is 25 turbidity grades equally divided from 1000-6000 NTU. Experimental results show that the training error with gradient feature in BP neural networks is 3%, and the training error with frequency spectrum features in BP neural networks is 5%. The error of turbidimeter used in establishment of a standard comparison library is 5%, so the maximum error is not more than 10%. Zhang [37] also demonstrates that extracting image gradient features as input to a neural network can improve the accuracy of detecting turbidity in this method. In short, state-of-the-art results can be obtained by combining traditional feature extraction and neural networks, and we can extract more sensitive features to measure low turbidity range in the future.

2) INSPIRATION BY UNDERWATER IMAGE RESTORATION

Researchers are devoted to restoring clear images from underwater images with high turbidity [38]. Turbidity detection can be inspired by this restoration of underwater turbidity images. These studies aim to establish the correspondence between clear images and turbidity images through image features, and once the corresponding relationship is established, it can be applied to the turbidity detection based on underwater images by changing the position relation between independent variables and dependent variables. In short, if we can recover original images from underwater images with high turbidity, we detect the difficulty degree of restoring original images from underwater images, and then we can build a relationship between restoration difficulty degrees and turbidity levels. For example, AMBE (absolute mean brightness error) is a performance index to restore turbidity image to clear image, and represents the average pixel distance of current brightness from the original brightness, i.e., the pixel difference of the average level of intensity in the new and original grayscale image. If the standard of a clear image is set, AMBE value of restoring the turbidity image to this standard clear image corresponds to the turbidity of the original image.

O'Byrne *et al.* [39] had built an open source library called underwater lighting and turbidity image library (ULTIR) to explore the relationship between underwater visibility and the performance of computer vision methods. According to the performance change rules of some algorithms, such as edge, color, and texture features under different turbidity levels, we can reverse the turbidity level of these algorithms

when they reach a performance threshold. Nevertheless, these laws are based only on three turbidity levels in ULTIR. Rodrigues *et al.* [40] studied how to enhance underwater images from low turbidity to high turbidity. According to the comparison between brightness and color saturation of the images under different turbidity levels, we can also establish the corresponding relationship between the feature change and the turbidity level.

3) SUMMARY

Because turbidity detection based on underwater image requires special light source, these methods are not the same as sampled images in which the solar light or the light source from a smartphone flash can be used. An uncontrollable light source and background, and the arbitrary scattering of light source will all affect imaging quality, so our possible directions include:

- Inspired by the turbidity detection method based on sampled images, we can build an underwater container with a function of automatic water absorption, drainage, and cleaning, so as to carry on the image acquisition in fixed area or fixed background for long-time span.
- Inspired by the underwater image restoration, or inspired by quantitative analysis the relationship between clarity levels of images and the difficulty degrees of image restoration in image processing, such as image denoising, image enhancement, blurred image reconstruction, etc., we can get the corresponding relationship between restoration difficulty degrees and turbidity levels.

C. WATER SURFACE IMAGE

With the popularity of smartphones, cameras, surveillance videos, and other imaging devices, the turbidity detection method based on the water surface image is a low-cost, efficient, and convenient method. This method not only benefits environmental scientists, river basin managers, and civil engineers, but also allows each citizen to care about the changes in water quality around them, so especially smartphones are the most meaningful source of images for this approach. Furthermore, as UAVs and robots are increasingly used by governments and companies, we can carry cameras on these devices to collect images for turbidity detection. Because this method has real-time performance and wide-space coverage, the application prospect of this method is also very considerable.

1) COLOR

Water surface images are susceptible to light intensity and shooting angle, so color is a significant but unstable image feature. Therefore, the combination of bands is necessary. Mizutani and Saito [41] proposed a turbidity alarm method using RGB reflectivity. The system consists of a camera and an image processing unit. The technical framework is also divided into five modules. Firstly, image preprocessing mainly includes RGB balance correction, which is to avoid the impact of different shooting angles on the experimental results. Secondly, the standard comparison library is still using the turbidity value measured by turbidimeter. Finally, the curve fitting relationship between the standard comparison library and the amplitude features of each band is established. The limitation of this method is that if the color of object region is the same as the color of surrounding areas, turbidity value can be not accurately measured, because the final results are judged according to the difference of the RGB reflectivity of each area.

The use of smartphones is more frequent and common than cameras, and the method of detecting turbidity directly by shooting on a smartphone makes this technique more popular. Leeuw and Boss [42] presented a turbidity detection method based on the smartphone with an application called HydroColor. The basic principle is to estimate the water turbidity by measuring the RGB reflectivity of the water surface. The system mainly includes 18% reflectivity gray cards, and smartphones with camera and HydroColor application. HydroColor uses the digital camera of smartphone as the radiation measuring instrument of three RGB bands, and the gray card is used to measure the reflectivity of sunlight to avoid interference of different sunlight intensity at different times.

The technical framework of turbidity detection function in HydroColor also includes the steps of image feature extraction, standard comparison library establishment, corresponding relationship establishment, and turbidity discrimination. Image features are measured by measuring the ratio of RGB reflectivity between the sky, gray card, and water surface. The standard comparison library refers to the measured value by turbidimeter, and then establishes the relationship between the measured value and the reflectivity. The experimental results show that the relationship is approximately linear in the low turbidity range, i.e., $\text{turbidity} = 1.06R_{rs}(green)$, and the fitting relation is a power exponential function in the high turbidity range, i.e., $\text{turbidity} = 22.57R_{rs}(Red)/(0.44 - R_{rs}(Red))$, where $R_{rs}(green)$ and $R_{rs}(Red)$ refers to the water remote sensing reflectivity of green and red band, respectively, measured by HydroColor. The experimental results also show that the exponential model is more suitable for different turbidity range detection, and the error of this model is 24%. Smartphones have been widely used as on-site optical instruments for water quality monitoring. This method extracts features by quantifying the irradiance levels of RGB reflectivity [13].

In short, the above methods are portable and real-time detection methods, but only a small range of turbidity information can be obtained. Real-time and large-scale turbidity information can also be obtained based on computer vision technology. The use of UAVs for low-altitude shooting can be very effective to break the space limit, but the difficulty of this method is that it needs to carry a camera on the drone, and obtain the actual measured turbidity values at the same time to establish a standard comparison library. By manually launching a small UAV carrying multi-spectral imaging sensors (height below 200m, resolution is

0.2m/ pixels), Vogt and Vogt [43] got the light reflection intensity of the NI (near infrared) light and the RGB bands of water surface. The extracted feature is the proportion relationship of light reflection intensity between B component after RGB decomposition and NI light. After determining the turbidity grade measured by the Secchi method [44], a look-up table is used to establish the relationship model.

Lim *et al.* [45] also proved that it is feasible to use UAVs to carry out digital cameras to detect turbidity. Image features are obtained with digital number, which is also an alternative to RGB reflectivity. It uses the correspondence between the low-altitude images and the turbidity values measured by turbidimeter as the raw data and standard comparison libraries. Then, the polynomial relationship between the reflected intensity of the three RGB bands and the measured values is finally established after brightness correcting of images taken at different angles. Nevertheless, Goddijn and White [46] presented that there is a strong linear relationship between RGB reflectivity and water quality parameters, e.g., yellow substances. Carder *et al.* [47] also used RGB reflectivity features to obtain the turbidity degree, which shows that when there are algae and debris in the water, the reflectivity of B band is greater than that of R band and G band; but when the oblique reflection is caused by the bottom topography, the reflectivity of B band is rather smaller.

2) GRAY

Compared with the color features, the gray features of water surface images have less dimensions to obtain enough information, but this feature is less affected by the change of external environment. Gao *et al.* [48] proposed a method based on image gray levels to judge whether the turbidity of sewage exceeds the standard. The basic principle is that the dark area in sewage images with suspended solids is larger than that in clean water images. Meanwhile, the whole system includes embedded system platform and image sensors. The obtained sewage image determines the object region by edge detection, and then performs grayscale processing. Moreover, the image is to be enhanced and the gray value of suspended objects in the image is increased by giving a greater weight to these areas with low gray value. Finally, the averaged gray value is the feature to be extracted. Because it is only to judge whether the sewage is qualified or not, and the corresponding relation is only comprised with the threshold value, the accuracy of this method is very low, but it has the characteristics of low power consumption and high convenience.

3) SUMMARY

There are many influence factors of turbidity detection based on water surface images. For example, it is difficult to control the intensity of the light source and the angle of light incidence, it is difficult to ensure good angle of shooting, and it is easy to be affected by the background such as water ripple. However, this method is of great significance, e.g., smartphones can be used to detect the turbidity of water around us at any time, the popularity of surveillance cameras leads to a great change in long time detection of water quality, and UAVs can carry a camera equipment to draw turbidity distribution map.

Besides, due to the easy acquisition of water surface images, we can get a large number of image datasets. For this reason, we can get a good correspondence model by training deep neural network. Khairi *et al.* [49] proposed a turbidity detection system based on feed-forward neural network with double hidden layers. The neural numbers of hidden layers is 20∗10, which has achieved good results in the turbidity detection of pipeline water. The input data of the system are arranged by an optical tomography system in the pipeline, which is obtained through multiple sets of transmitting and receiving terminals.

Therefore, we also have the following tasks to ensure that the turbidity detection system based on water surface images can achieve better accuracy.

- Studying the more sensitive and robust combination of RGB band reflectivity, and using other color spaces which are less sensitive to luminance changes, such as HSV (Hue, Saturation, Value) color space.
- Studying a deep neural network model based on a large number of image training. The classification label can be set to turbidity levels to facilitate the establishment of a standard comparison library. This method can be applied in smartphones and surveillance cameras where the trained model is placed on the server.

D. INVISIBLE LIGHT IMAGE

In the turbidity detection method based on computer vision, the way of using cameras to identify the image has the advantages of high convenience, low cost and easy popularization. However, the proportion of wave range of visible light in the whole spectrum is very small, and many researchers are devoted to establishing relation models between turbidity and other invisible light features, such as infrared images and hyperspectral images, which have been widely used in turbidity detection. The purpose of this section is to provide inspiration for feature combinations, model selection, and accuracy improvements in visible light images.

1) INFRARED IMAGE

Infrared light is less susceptible to attenuation than visible light, so ROI where features can be detected can become larger, but this method requires an additional infrared receiving device. Hussain and Nath [50] proposed a typical and convenient turbidity detection method based on infrared radiation (IR). The main equipment of their system includes smartphone, infrared LED lamp, plane concave lens, plastic bracket, and sample container. In this system, infrared LED lamp is powered by smartphone, and the infrared ray emitted by infrared LED lamp is vertically irradiated to the sample through a plane concave lens. Meanwhile, infrared receiver in the smartphone receives 90 degrees of scattering light from the sample through a small hole. Finally, the received infrared radiation intensity is used as extracted feature value.

Experiments show that the measured value is linearly related to the infrared radiation intensity. The weight of whole system is only about 250 gram.

The infrared receiver can also be loaded on the drone to detect a wide range of turbidity in real time. Vogt and Vogt [43] used small UAVs to obtain the light reflectivity of near infrared radiation (NIR) and RGB band at the same time, and then extracted the proportion of the B band component and NIR intensity, so as to establish look-up table between the feature and measured value. Khairi *et al.* [49], [51] presented a method based on a neural network model for turbidity detection. The data sources of these methods are all collected through multiple sets of IR transmitters and receivers. Postolache *et al.* [52] also proposed a neural network model method based on the different locations of IR emitter to build training dataset.

2) REMOTE SENSING IMAGE

Since satellite remote sensing technology has the advantages of fast, economical, and extensive coverage, remote sensing images are widely used in countries around the world for large-scale water quality measurement, including turbidity detection [53]–[55]. The main idea of this method is to use remote sensing data, including different spatial resolution, time span, and spectral band, carried by various sensors and satellites to establish a remote sensing inversion algorithm between the optical features and water quality parameters measured at the same time [56]. Because the spectral characteristics of the turbidity of the water quality can be detected by satellite sensors, there are many studies on the inversion model to detect turbidity based on remote sensing images [57].

These studies try to find the relationship model between turbidity and reflectivity of each band in remote sensing data. The inversion models include the empirical model, semi-empirical model, physical model, neural network model, etc. Qiu *et al.* [58] analyzed the relationship between the reflectivity of several bands and the turbidity value, and established a polynomial exponential relationship between the multi-band reflectivity and turbidity, in which the wavelength data come from the Geostationary Ocean Color Imager (GOCI). Ahmed *et al.* [71] evaluated turbidity by using single-band turbidity retrieval algorithm, which built a normalized difference vegetation index (NDVI), and the data came from Landsat 8 OLI (Operational Land Imager). Constantin *et al.* [72] used 12 years of remote sensing data to calculate the turbidity of the water surface and set up an exponential model between the turbidity and the remote sensing reflectance of the 645nm wave, and the information comes from the MODIS. In conclusion, the remote sensing data from the GOCI, MODIS, and Landsat series are commonly used for turbidity detection. In Table 3, some sensor types, application fields, and measurement ranges are given, which indicates that turbidity detection methods based on remote sensing images have been widely used all over the world for a long time, and provides a theoretical guidance for the use of computer vision technology to detect turbidity. In recent years, deep neural network models have been playing an important role in computer vision algorithms, which is also applied to remote sensing images [73], [74].

3) SUMMARY

Water with different turbidity has different light reflectivity in certain bands, which are features that needs to be discovered and extracted. There is a statistical relationship or a relationship which is similar of hash tables between turbidity and reflectivity of these invisible wavelengths. This regularity allows us to establish the inversion model to estimate turbidity value according to real-time reflectivity. However, the main problem of remote sensing image detection is the need for atmospheric correction [75]. Further, existing researches show that the combination of different bands, such as addition or ratio relationship, is more robust than relationship between turbidity and single-band feature. This combination method has been practiced in remote sensing images [58], and a more robust model has been obtained at infrared wavelengths, whether it is simple NI light [50], or the combination of NI and RGB bands [43]. Based on the above facts, we believe that:

- Turbidity detection method based on computer vision is theoretically proved to be robust, which is based on the regular change of light reflectivity in different turbidity degree.
- During the feature extraction of the image, we can find the most sensitive feature of the turbidity change from the combination of the visible light band (e.g., the combination of RGB reflectivity and other color spaces) to improve the precision.
- Inspired by the combination of near infrared light and RGB band, other invisible bands can also be combined with visible bands for feature extraction.

IV. DISCUSSION

First of all, the turbidity range of typical water body is described as follows. The turbidity of drinking water is less than 10 NTU [76], which is close to that of clear lake water, such as 89% of Finnish lake waters [29]. For this type of water body, a measurement method with low range and high precision is required. In addition, the turbidity range of streams, rivers and lakes is between 0-400 NTU [76], which requires a medium range method. For agricultural farming and erosion areas, the maximum turbidity range can be close to 1000 NTU [76]. For sewage, the turbidity range can reach thousands of NTU [36]. In the latter two cases, a measurement method that requires large range is required for this type. The turbidity measurement range of turbidimeter covers 0-10000 NTU [21], and the inversion method based on remote sensing images can only guarantee the lower root mean square error (RMSE) between the inversion value and the real value within 0-40 NTU range [62].

However, the existing research shows that the computer vision technology can be used to detect turbidity accurately

TABLE 3. Turbidity detection based on remote sensing images.

Year	Sensor	Country/Area	Range (NTU)	Research object	Reference
1993	IRS-1A-LISS-I	India	15-45	Tawa reservoir	[59]
1996	SPOT-HRV	France	3-15	Tuttel Creek Reservoir	[60]
2007	IKONOS	United States	2-6	Charles River, Boston	[61]
2008	MERIS	Europe	1-25	Cienfuegos Bay, Laucala Bay	[7]
2009	ALOS-AVNIR-2	Japan	<45	Penang, Malaysia	[62]
2010	MODIS-Aqua	United States	0.5-70	Biscay Bay	[63]
2012	MERIS	Europe	<60	Alqueva Reservoir	[64]
2013	MODIS	Israel	<10	Dead Sea	[65]
2014	GOCI	Republic of Korea	40-80	western coastal area of the Korean Peninsula	[66]
2015	MODIS	China	5.8-577.2	Estuary of Yangtze River and XuwenCoral Reef Protection Zone	[67]
2016	MODIS	Burkina Faso	10-927	Bagre Reservoir	[68]
2017	Landsat 8 sensor	Italy	1-200	Po River prodelta	[69]
2018	Landsat 8 sensor	Colombia	13.50-117.00	El Guajaro Reservoir	[70]

in the middle and high turbidity range. In Fig. 5(a), we compared eight turbidity detection methods based on computer vision, in which there is including one method of using the smartphone to detect infrared attenuation intensity. Meanwhile, three measurement ranges of the HACH 2100AN turbidimeter are used as a reference. In the low range, the

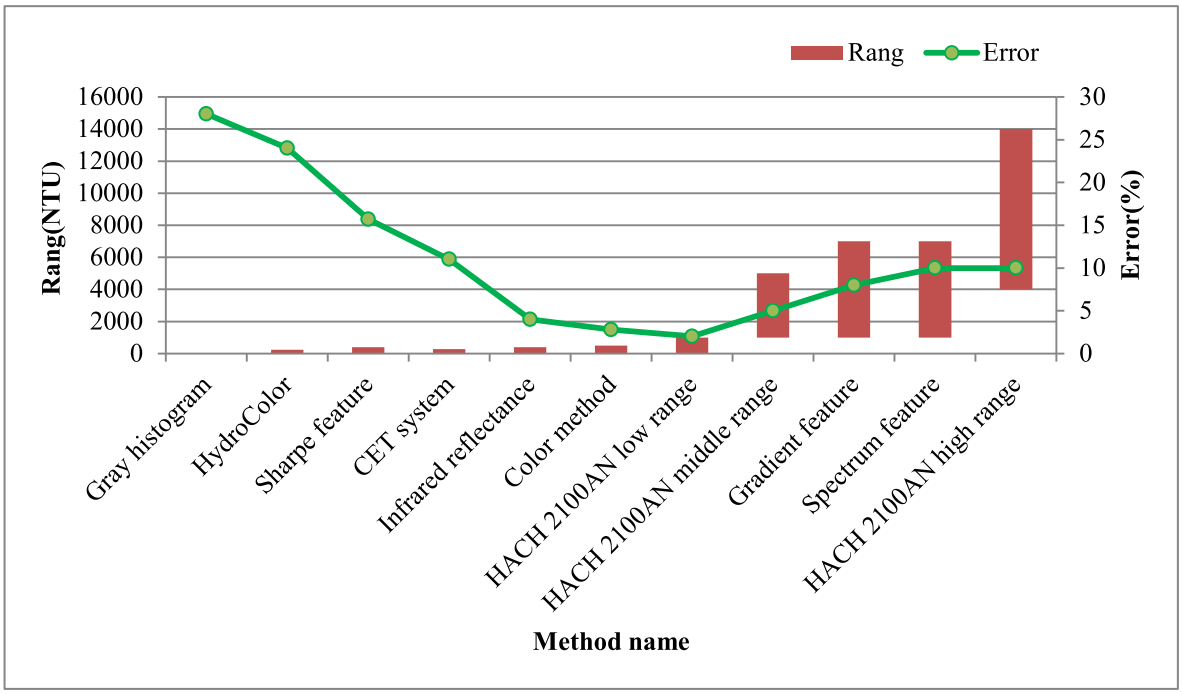

(a)

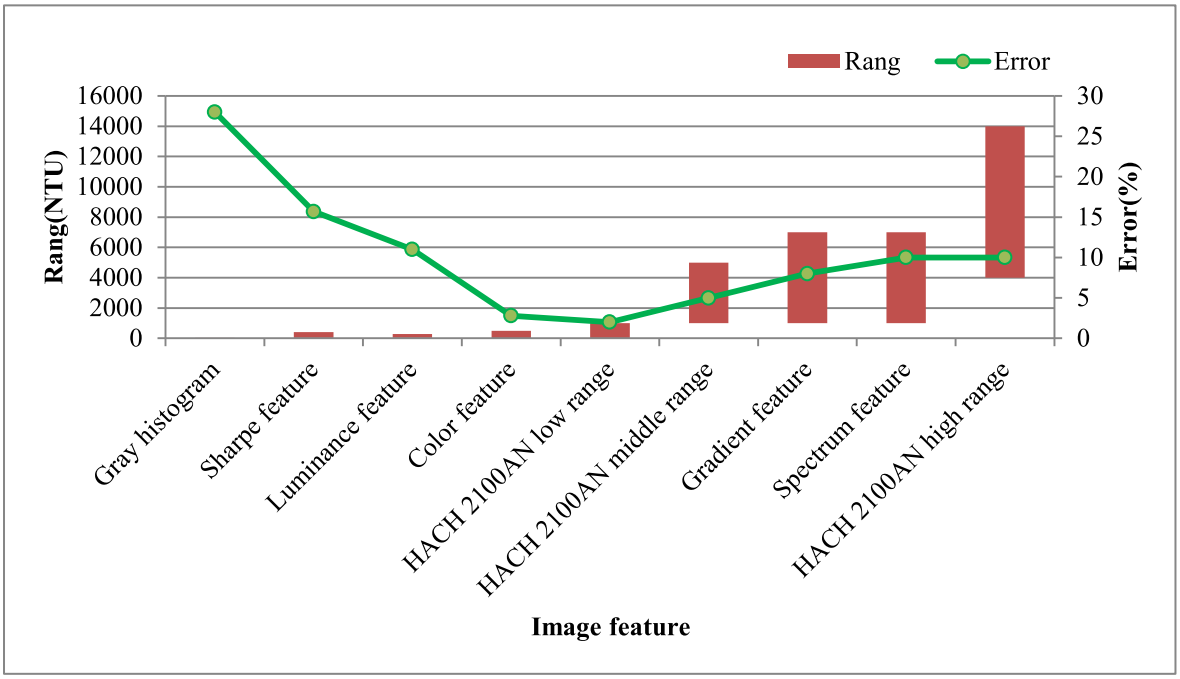

(b)

FIGURE 5. Comparison in different aspects of turbidity detection methods based on computer vision. (a) Range and error of typical image-based methods. (b) Range and error of image-based methods according to different image sources. (c) Range and error of image-based methods according to different image features.

resolution of turbidimeter is higher, and the error of image-based method is large, which can not meet the requirements of high precision and high resolution. Nevertheless, in the medium and high range, the error of the method based on color feature, gray gradient and frequency domain feature approaches the error of turbidimeter, which indicates that the turbidity detection methods based on computer vision can replace the turbidimeter in medium and high range.

According to the classification method of different image sources, we have chosen the method with the largest range

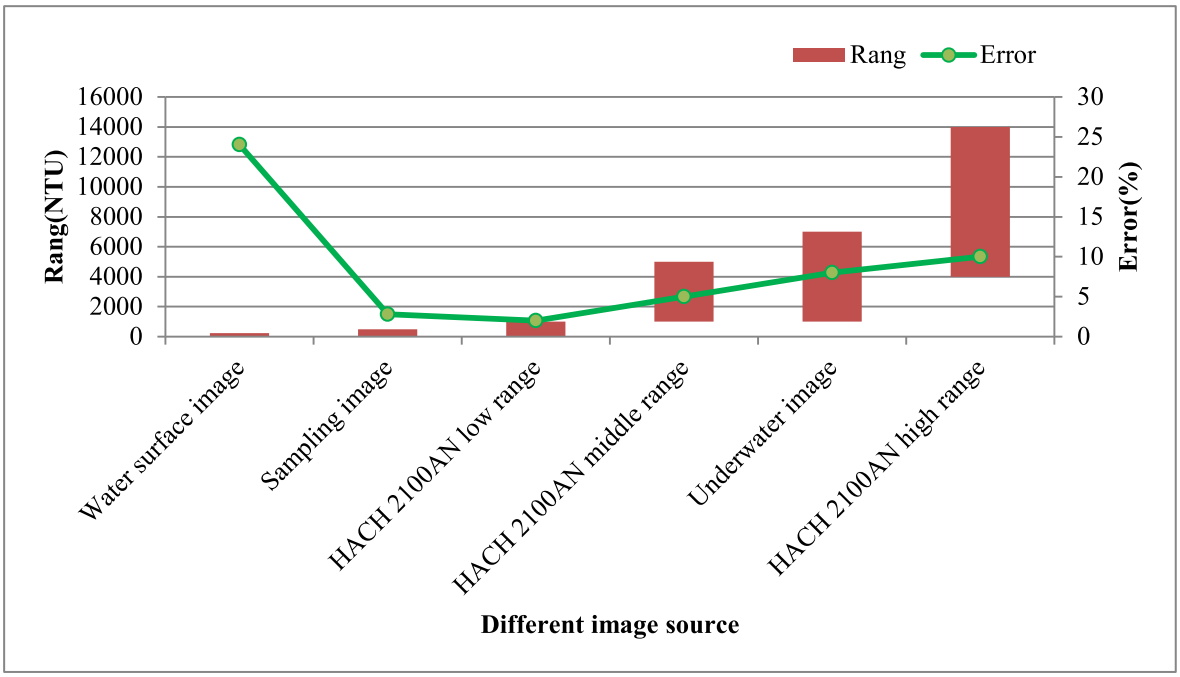

(c)

FIGURE 5. *(Continued.)* **Comparison in different aspects of turbidity detection methods based on computer vision. (a) Range and error of typical image-based methods. (b) Range and error of image-based methods according to different image sources. (c) Range and error of image-based methods according to different image features.**

in each image source for comparison, which is shown in Fig. 5(b). Even if the same feature extraction method is adopted, the difference of the image acquisition method will significantly affect the measurement range and accuracy. The error of sampling image method is the smallest, because it is easy to control light source, background, and feature selection methods. In the case of using a water surface image, because of the uncertainty of the incident angle, background, and shooting angle of the light source (e.g., sunlight), many image features are difficult to be extracted accurately. This method that only extracts a single image feature is poorly stable, so a variety of feature combinations or a large number of training models with different angles and backgrounds are the solutions to this problem. However, for the method based on water surface images, the resolution of turbidity can meet the wide application value and the significance of environmental protection as long as it reaches 1 NTU in low range. The method based on underwater measurement can be applied in high turbidity liquid, but the need of regular cleaning limits the application in the turbidity detection on the vertical surface of water body, and the key to meet this demand is to design an underwater automatic and real-time detection system.

For the turbidity detection methods or systems of these different image sources, we list the representative methods or system names in Appendix, and show the range, error, features, principle, relationship model, and main equipment of each method in detail. The disadvantages and future work are both pointed out. Their basic principles are similar, which is based on the relationship between the degree of light attenuation and the change of image features in different turbidity liquid. However, even with the same image features, different systems, image preprocessing, and model selection will result in differences in range and accuracy. Fig. 5(c) shows the contrast of seven image features. The method based on the reflection intensity of the RGB bands (i.e., color feature) in images can reach the minimum error and near the turbidimeter accuracy, because the combination of different wavebands is one of the key factors to reduce detection error. In addition, the method based on gray gradient and spectral energy information is of great application value in high turbidity range.

Note, we need to be aware that the upper limit of the turbidity of drinking water and lake water is very low [29]. However, the error of turbidity detection based on image recognition in low range is between 20% and 25%, and the resolution is generally only on the order of 1 NTU, which is much higher than 0.001 NTU in HACH 2100AN turbidimeter. Therefore, each module can be improved to achieve better accuracy and resolution. As shown in Table 4, we summarize the existing image-based methods of image preprocessing, feature extraction and relational modeling. There are a lot of image preprocessing algorithms and image feature extraction algorithms, but there are few methods used now. These methods are more advantageous if there are not very sensitive to image luminance changes (e.g., band decomposition and combination).

TABLE 4. Operation method in existing researches.

Module	Operation
Image preprocessing	Image denoising, image enhancement, image segmentation
Image feature	Luminance, color, shape, grayscale gradient, grayscale extreme value and distribution, grayscale histogram, frequency domain information
Relationship model	Linear relationship, polynomial relationship, power relationship, neural network model

Currently, researchers widely use invisible images, especially remote sensing images, to detect large-scale water quality data including turbidity. The problem with this method is that it is difficult to obtain real-time data, difficult to be popularized and difficult to detect the turbidity of a fixed location or a sample. Besides, because of atmospheric interference, its accuracy and resolution are unlikely to reach the level of the turbidimeter. However, we can get inspiration from the image band combination, the inversion model establishment, and the neural network algorithm of this method. For example, the deep neural network model is very impressive for improving the accuracy of this method. For discrete classification using neural networks, continuous turbidity values can be obtained by adding a linear map in the last layer, but this also requires a large enough annotated dataset to support these researches. In particular, high- precision model training of large standard comparison libraries based on convolutional neural networks [77] and real-time detection of turbidity based on recurrent neural networks [78] and surveillance video are feasible.

V. CONCLUSION AND FUTURE WORK

This paper reviewed the existing researches on turbidity detection based on computer vision, and summarized the principle, range, error, feature extraction, relationship model, system equipment, deficiency, and technical framework of these typical methods. In this review, the image-based turbidity detection methods were divided into four categories according to different image sources, and seven image features extracted in these studies were also pointed out. This review described a common principle and necessary system equipment of existing researches, built a unified technical framework, found out existing problems, and directed future work on systems, algorithms, and unified standards.

Based on the analysis of existing work, image-based turbidity detection methods can reach the same accuracy of turbidimeter in medium and high range, which suggests that this technology can be applied in some scenarios such as wastewater classification, replacing expensive, fragile, and difficult to operate turbidimeter. However, in the turbidity detection of low range such as drinking water and clear lake water, it is necessary to further improve in imaging systems, feature extraction, and modeling algorithms to improve accuracy and resolution.

In this paper, we provided a comparison and framework to find better feature extraction and modeling methods, and we also presented state-of-the-art turbidity detection methods based on computer vision, which balance cost, convenience, and space-time coverage. Finally, we should pay more attention to the following aspects in the future work:

- System. In order to get higher quality images, we can improve the quality of light source, increase the background comparison, and use better imaging equipment (e.g. CCD or CMOS, high resolution camera, etc.). Another important aspect is to get images from different angles, and then combine the features of these angles. We can also design more automated systems to achieve detection automation, such as automatic sampling, drainage, cleaning, etc. In short, it is very important to capture images in a controlled environment.
- Algorithm. Firstly, we can pay attention to the work of image preprocessing, e.g., image brightness correction, image enhancement, image denoising, and image segmentation, etc. In feature extraction module, we can combine multiple features including the combination of light reflectivity of each band. We can also try other color spaces that are less impacted to light, e.g., HSV. In relationship model building module, we can try deep neural network model, e.g., CNN and RNN.
- Unified standards. The unified standards include a unified standard comparison library, a unified imaging protocol, etc. The standard comparison library can be accomplished by establishing a global or multi-regional standard for different water quality in the world. A unified protocol of resolution, storage, and transmission of images can be established, and software can also be developed to increase the resolution and reproducibility of turbidity detection.

APPENDIX

See Table 5.

TABLE 5. Details of typical turbidity detection methods based on computer (Range and accuracy according to the experimental data or conclusion in references).

Image source	Typical method or system	Range (NTU)	Error (%)	Principle	Feature	Model	Main equipment of system	Disadvantages	Future work	Ref.
Sample image	CET	30-250	10	The light passing through different turbidity liquids will undergo different degrees of attenuation due to scattering, transmission, and absorption.	The number of pixels within the range of luminance threshold	Linear relationship between the number of pixels that the incident light attenuates to 63% and the measured value with spectrophotometer	4 L glass vessel, IR light source, 1.2M pixel monochrome CMOS camera, stirrer	1. large errors will occur when the measurement is less than 30 NTU 2. it is affected by the peak of luminance intensity 3. no auxiliary equipment is used to clean the container automatically	1. increase light intensity can reduce the lower range limit of measurement 2. increase the image preprocessing operation such as image segmentation, and train a good classifier to get ROI of the image. 3. add auxiliary equipment to ensure long-time deployment	[26]
	Secci-3000	<7	3.8(in high range)-20(in low rang-e)	The difference of attenuation degree of light passing through different turbidity liquids at same distances.	The reflectivity difference of the same color at different depths.	Linear relationship between different reflectivity and laboratory measured value	Smartphones with MA application, Secci3000, server	1. the upper limit of measurement range is low 2. accuracy is affected by sample color, light intensity and smartphone type	1. increase the light path length (ROI) of the device when shooting 2. improve the quality of light source 3. set up an imaging and transmission protocol, and a user's manual	[29]
	Shape feature	20-380	15.7	The clarity of the bottom in different turbidity samples is different	The number of rings that can be detected at the container bottom	Linear relationship and logarithmic function between the number of rings and the measured value with laboratory instrument.	Sample container, light source, image processing unit, and bracket with rings at the bottom	1. resolution of the camera affects circular detection 2. robustness of circular detection algorithm affects experimental accuracy.	1. increase the resolution of cameras 2. image preprocessing and robust circular detection algorithm selection 3. developing a portable equipment	[33]
	Infrared radiation intensity	0-400	6.5 in maxim-um, less than 2 in general	The IR scattering degree of samples with different turbidity is different	The intensity of infrared radiation after 90 degree scattering through liquid.	Linear relationship between infrared radiation intensity and laboratory measurement	Smartphone with meter and StanXY application, infrared LED lamp, plane concave lens, container	1. it costs 86 dollars exceeding the price of the smartphone	1. the accuracy can reach 0.1 NTU, and further improvement can approach the instrument level 2. applications in clinical and biological investigations	[50]
	Gray histogra-m feature	5-15	<28	The maximum gray and distribution of samples with different turbidity are different.	Grayscale extremum in 120-180 pixel range of gray histogram	The corresponding look-up table of the image gray value and the laboratory measurement	Camera, light source, fully transparent container, computer	1. low precision 2. the standard comparison library has few data	1. enhancing image preprocessing 2. enlarging the standard comparison library dataset 3. improvement of light source instead of sunlight	[34]
	Color feature	1-500	2.8	The attenuation of RGB reflectivity in	The reflectivity difference of B band and	The polynomial relation between the feature difference and the measured	CCD camera, light source, filter, sample feeder, computer	1. the reflectivity of the B band occasionally appears singular	1. improve the quality of light source	[25]

TABLE 5. *(Continued.)* **Details of typical turbidity detection methods based on computer (Range and accuracy according to the experimental data or conclusion in references).**

				different turbidity liquids is different after transmission	G band in different turbidity	value with turbidimeter		value		
Under water image	Gray and gradient features	1000-6000	8	The difference between the gray level and the spatial gradient of the light passing through the liquid with different turbidity.	Gray energy, gradient energy, gray entropy, gradient entropy, gray variance and gradient variance.	B-P neural network model with 4 hidden layers, and each layer includes 10 neurons	Underwater light source, underwater camera, image processing terminal	1. the operation time of this method is higher than that based on spectrum.	1. when using external power supply, the gradient information can be extracted, so that the system is in a high performance state.	[36]
	Frequency domain features	1000-6000	10	The spectral characteristics of light passing through different turbidity liquids are inconsistent	Image energy on horizontal component, vertical component and diagonal component	B-P neural network model with 4 hidden layers ,and each layer includes 10 neurons	Underwater light source, underwater camera, image processing terminal	1. the precision is lower than the method based on the spatial gradient	1. when the battery is used as an energy source, the spectrum information can be extracted, and the system runs in the state of low power state	[36]
Water surface image	HydroColor	0-240	24	Water surface with different turbidity have different RGB reflectivity	The ratio of RGB reflectivity between the sky, gray card, and water surface	Power function relation between reflectivity and measurement value	Smartphone with Color application, 18% reflectivity gray card	1. RGB reflectivity will be impacted by the depth of water 2. good shooting angle is 40 to 135 degrees, best angle of sunlight is 15 to 60 degrees	1. other water quality parameters can be estimated by using combination or ratio of RGB reflectance in this method	[42]

REFERENCES

[1] A. F. B. Omar and M. Z. B. Matjafri, "Turbidimeter design and analysis: A review on optical fiber sensors for the measurement of water turbidity," *Sensors*, vol. 9, no. 10, pp. 8311–8335, 2009.

[2] B. G. B. Kitchener, J. Wainwright, and A. J. Parsons, "A review of the principles of turbidity measurement," *Progr. Phys. Geograph., Earth Environ.*, vol. 41, no. 5, pp. 620–642, 2017.

[3] B. Yan, K. Stamnes, M. Toratani, W. Li, and J. J. Stamnes, "Evaluation of a reflectance model used in the SeaWiFS ocean color algorithm: Implications for chlorophyll concentration retrievals," *Appl. Opt.*, vol. 41, no. 30, pp. 6243–6259, 2002.

[4] N. G. Maksimovich, V. T. Khmurchik, and A. D. Demenev, "The role of microorganisms in elevating the turbidity of dam seepage water," *Power Technol. Eng.*, vol. 50, pp. 6–8, May 2016.

[5] J. Michaud, "A citizen's guide to understanding & monitoring lakes and streams," in *Envirovision-Environmental Consulting Service*. Puget Sound Water Quality Authority, 1991.

[6] S. A. P. Ruturaj and S. Jamale, "Turbidity measurement using video camera," *Int. J. Elect., Electron. Comput. Syst.*, vol. 2, no. 3, 2014.

[7] O. Sylvain *et al.*, "Optical algorithms at satellite wavelengths for total suspended matter in tropical coastal waters," *Sensors*, vol. 8, no. 7, pp. 4165–4185, 2008.

[8] M. Metzger *et al.*, "Low-cost GRIN-lens-based nephelometric turbidity sensing in the range of 0.1–1000 NTU," *Sensors*, vol. 18, no. 4, p. 1115, 2018.

[9] C. Joannis, G. Ruban, M.-C. Gromaire, J.-L. Bertrand-Krajewski, and G. Chebbo, "Reproducibility and uncertainty of wastewater turbidity measurements," *Water Sci. Technol.*, vol. 57, no. 10, pp. 1667–1673, 2008.

[10] C. Lu and X. Tang, "Surpassing human-level face verification performance on LFW with GaussianFace," in *Proc. 29th AAAI Conf. Artif. Intell. (AAAI)*, 2015, pp. 3811–3819.

[11] J. Janai, F. Güney, A. Behl, and A. Geiger. (2017). "Computer vision for autonomous vehicles: Problems, datasets and state-of-the-art." [Online]. Available: https://arxiv.org/abs/1704.05519

[12] J. Wäldchen and P. Mäder, "Plant species identification using computer vision techniques: A systematic literature review," *Arch. Comput. Methods Eng.*, vol. 25, no. 2, pp. 507–543, 2018.

[13] L. Goddijn-Murphy, D. Dailloux, M. White, and D. Bowers, "Fundamentals of *in situ* digital camera methodology for water quality monitoring of coast and ocean," *Sensors*, vol. 9, no. 7, pp. 5825–5843, 2009.

[14] C. En, Z. Rong-Xin, and Y. Fei, "Automatic detection and assessment system of water turbidity based on image processing," *Indonesian J. Elect. Eng.*, vol. 11, no. 3, pp. 1506–1513, 2013.

[15] H. Lu, Y. Li, S. Nakashima, and S. Serikawa, "Turbidity underwater image restoration using spectral properties and light compensation," *IEICE Trans. Inf. Syst.*, vol. E99.D, no. 1, pp. 219–227, 2016.

[16] R. E. Villar *et al.*, "A study of sediment transport in the Madeira River, Brazil, using MODIS remote-sensing images," *J. South Amer. Earth Sci.*, vol. 44, pp. 45–54, Jul. 2013.

[17] G. Wattelez, C. Dupouy, J. Lefèvre, S. Ouillon, J.-M. Fernandez, and F. Juillot, "Application of the support vector regression method for turbidity assessment with MODIS on a shallow coral reef lagoon (Voh-Koné-Pouembout, New Caledonia)," *Water*, vol. 9, no. 10, p. 737, 2017.

[18] X. Shen and Q. Feng, "Statistical model and estimation of inland riverine turbidity with Landsat 8 OLI images: A case study," *Environ. Eng. Sci.*, vol. 35, no. 2, pp. 132–140, 2018.

[19] G. J. Telesnicki and W. M. Goldberg, "Comparison of turbidity measurement by nephelometry and transmissometry and its relevance to water quality standards," *Bulletin Marine Sci.*, vol. 57, no. 2, pp. 540–547, 1995.

[20] A. I. Dogliotti, K. G. Ruddick, B. Nechad, D. Doxaran, and E. Knaeps, "A single algorithm to retrieve turbidity from remotely-sensed data in all coastal and estuarine waters," *Remote Sens. Environ.*, vol. 156, pp. 157–168, Jan. 2015.

[21] Hach Company, USA. (2010). *Turbidimeter Instruction Manual*. [Online]. Available: https://www.Hach.com

[22] L. Han, "Spectrometry of turbidity in surface water," in *Proc. Int. Geosci. Remote Sens. Symp.*, vol. 2, May 1996, pp. 1395–1397.

[23] R. J. Davies-Colley and D. G. Smith, "Turbidity suspeni)ed sediment, and water clarity: A review1," *J. Amer. Water Resour. Assoc.*, vol. 37, no. 5, pp. 1085–1101, 2001.

[24] A. Beer, "Bestimmung der absorption des rothen lichts in farbigen flüssigkeiten," *Annalen der Physik*, vol. 162, no. 5, pp. 78–88, 1852.

[25] Q. Q. Wang, L. I. Xu-Yu, and M. L. Zhang, "Different turbidity fast detection technology based on CCD," *Instrum. Technique Sensor*, 2013, pp. 97–101.

[26] D. Mullins, D. Coburn, L. Hannon, E. Jones, E. Clifford, and M. Glavin, "A novel image processing-based system for turbidity measurement in domestic and industrial wastewater," *Water Sci. Technol.*, vol. 77, no. 5, pp. 1469–1482, 2018.

[27] F. N. Hamidi, M. F. Zainuddin, Z. Abbas, and A. F. Ahmad, "Low cost and simple procedure to determine water turbidity with image processing," in *Proc. Int. Conf. Imag., Signal Process. Commun.*, 2017, pp. 30–34.

[28] T. Toivanen, S. Koponen, V. Kotovirta, M. Molinier, and C. Peng, "Water quality analysis using an inexpensive device and a mobile phone," *Environ. Syst. Res.*, vol. 2, pp. 1–6, Dec. 2013.

[29] T. Näykki, S. Koponen, T. Väisänen, T. Pyhälahti, T. Toivanen, and I. Leito, "Validation of a new measuring system for water turbidity field measurements," *Accreditation Qual. Assurance*, vol. 19, no. 3, pp. 175–183, 2014.

[30] J. Pitarch, "Biases in ocean color over a secchi disk," *Opt. Express*, vol. 25, no. 24, pp. A1124–A1131, 2017.

[31] M. Pilz, S. Honold, and A. Kienle, "Determination of the optical properties of turbid media by measurements of the spatially resolved reflectance considering the point-spread function of the camera system," *J. Biomed. Opt.*, vol. 13, no. 4, p. 054047, 2008.

[32] R. S. Jamale and S. A. Pardeshi, "Turbidity measurement using video camera," *Int. J. Electr., Electron. Comput. Syst.*, vol. 2, no. 3, 2014.

[33] M. M. E. Chai, S. M. Ng, and H. S. Chua, "An alternative cost-effective image processing based sensor for continuous turbidity monitoring," in *Proc. Asian Conf. Chem. Sensors*, 2016, p. 020014.

[34] V. Karnawat and S. L. Patil, "Turbidity detection using image processing," in *Proc. Int. Conf. Comput., Commun. Autom.*, Apr. 2017, pp. 1086–1089.

[35] S. W. Effler, D. M. O'Donnell, F. Peng, A. R. Prestigiacomo, M. Perkins, and C. T. Driscoll, "Use of robotic monitoring to assess turbidity patterns in Onondaga Lake, NY," *Lake Reservoir Manage.*, vol. 22, no. 3, pp. 199–212, 2006.

[36] A. Li, "Design and implementation of turbidity detection system based on image recognition," Harbin Inst. Technol., Harbin, China, Tech. Rep., 2013.

[37] X. Zhang, "Water quality turbidity detection based on image recognition system design and implementation," *Adv. Intell. Syst. Comput.*, vol. 613, pp. 63–70, Sep. 2018.

[38] T. Haware and R. Gumble, "A review on underwater image scene enhancement and restoration using image processing," *Int. J. Innov. Res. Elect., Electron., Instrum. Control Eng.*, vol. 5, no. 9, pp. 28–31, 2017.

[39] M. O'Byrne, F. Schoefs, V. Pakrashi, and B. Ghosh, "An underwater lighting and turbidity image repository for analysing the performance of image-based non-destructive techniques," *Struct. Infrastruct. Eng.*, vol. 14, no. 1, pp. 104–123, 2017.

[40] D. D. D. O. Rodrigues, W. F. de Barros, J. P. de Queiroz-Neto, A. G. Fontoura, and J. R. H. Carvalho, "Enhancement of underwater images in low-to-high turbidity rivers," in *Proc. 29th SIBGRAPI Conf. Graph., Patterns Images*, Oct. 2016, pp. 233–240.

[41] Y. N. N. Mizutani and K. Saito, "Realtime monitoring of turbid water by using video camera, personal computer and image processing," Asia Air Survey, Japan, Tech. Rep., 1988.

[42] T. Leeuw and E. Boss, "The hydrocolor app: Above water measurements of remote sensing reflectance and turbidity using a smartphone camera," *Sensors*, vol. 18, no. 1, p. 256, 2018.

[43] M. C. Vogt and M. E. Vogt, "Research article: Near-remote sensing of water turbidity using small unmanned aircraft systems," *Environ. Pract.*, vol. 18, no. 1, pp. 18–31, 2017.

[44] Z. Lee *et al.*, "Secchi disk observation with spectral-selective glasses in blue and green waters," *Opt. Express*, vol. 25, no. 17, pp. 19878–19885, 2017.

[45] H. S. Lim, M. Z. Matjafri, and K. Abdullah, "Algorithm for turbidity mapping using digital camera images from a low-altitude light aircraft," in *Proc. IEEE Int. Conf. Comput. Sci. Inf. Technol.*, Aug. 2009, pp. 200–204.

[46] L. M. Goddijn and M. White, "Using a digital camera for water quality measurements in Galway Bay," *Estuarine Coastal Shelf Sci.*, vol. 66, pp. 429–436, Feb. 2006.

[47] K. L. Carder *et al.*, "Illumination and turbidity effects on observing faceted bottom elements with uniform Lambertian albedos," *Limnol. Oceanogr.*, vol. 48, pp. 355–363, Jan. 2003.

[48] M. Gao, J. Tian, L. Ai, and F. Zhang, "Sewage image feature extraction and turbidity degree detection based on embedded system," in *Proc. Int. Conf. Multimedia Inf. Technol.*, Dec. 2008, pp. 357–360.

[49] M. T. M. Khairi, S. Ibrahim, M. A. M. Yunus, M. Faramarzi, and Z. Yusuf, "Artificial neural network approach for predicting the water turbidity level using optical tomography," *Arabian J. Sci. Eng.*, vol. 41, no. 9, pp. 3369–3379, 2016.

[50] I. Hussain, K. Ahamad, and P. Nath, "Water turbidity sensing using a smartphone," *RSC Adv.*, vol. 6, no. 27, pp. 22374–22382, 2016.

[51] O. A. Postolache, P. M. B. S. Girao, J. M. D. Pereira, and H. M. G. Ramos, "Multibeam optical system and neural processing for turbidity measurement," *IEEE Sensors J.*, vol. 7, no. 5, pp. 677–684, May 2007.

[52] O. Postolache, J. M. D. Pereira, P. S. Girao, and H. E. Ramos, "Smart flexible turbidity sensing based on embedded neural network," in *Proc. IEEE Conf. SENSORS*, Oct. 2006, pp. 658–661.

[53] S. Novoa *et al.*, "Atmospheric corrections and multi-conditional algorithm for multi-sensor remote sensing of suspended particulate matter in low-to-high turbidity levels coastal waters," *Remote Sens.*, vol. 9, no. 1, p. 61, 2017.

[54] X. Hou, L. Feng, H. Duan, X. Chen, D. Sun, and K. Shi, "Fifteen-year monitoring of the turbidity dynamics in large lakes and reservoirs in the middle and lower basin of the Yangtze River, China," *Remote Sens. Environ.*, vol. 190, pp. 107–121, Mar. 2017.

[55] S. Constantin, D. Doxaran, and Ş. Constantinescu, "Estimation of water turbidity and analysis of its spatio-temporal variability in the danube river plume (black sea) using MODIS satellite data," *Continental Shelf Res.*, vol. 112, pp. 14–30, Jan. 2016.

[56] L. Zheng, "Study on remote sensing algorithm and the temporal-spatial distributionof turbidity in the East China Seas," Nanjing Univ. Inf. Sci. Technol., Nanjing, China, Tech. Rep., 2017.

[57] F. N. Güttler, S. Niculescu, and F. Gohin, "Turbidity retrieval and monitoring of Danube Delta waters using multi-sensor optical remote sensing data: An integrated view from the delta plain lakes to the western–northwestern Black Sea coastal zone," *Remote Sens. Environ.*, vol. 132, pp. 86–101, May 2013.

[58] Z. Qiu, L. Zheng, Y. Zhou, D. Sun, S. Wang, and W. Wu, "Innovative GOCI algorithm to derive turbidity in highly turbid waters: A case study in the Zhejiang coastal area," *Opt Express*, vol. 23, no. 19, pp. A1179–A1193, Sep. 2015.

[59] V. K. Choubey, "Correlation of turbidity with indian remote sensing satellite-1A data," *Int. Assoc. Sci. Hydrol. Bull.*, vol. 37, pp. 129–140, 1993.

[60] D. G. Goodin, J. A. Harrington, Jr., M. D. Nellis, and D. C. Rundquist, "Mapping reservoir turbidity patterns using SPOT-HRV data," *Geocarto Int.*, vol. 11, no. 4, pp. 71–78, 1996.

[61] F. L. Hellweger, W. Miller, and K. S. Oshodi, "Mapping turbidity in the Charles River, Boston using a high-resolution satellite," *Environ. Monit. Assessment*, vol. 132, pp. 311–320, Sep. 2007.

[62] H. S. Lim, M. Z. Matjafri, and K. Abdullah, "Turbidity measurement from ALOS satellite imagery," in *Proc. OCEANS*, May 2009, pp. 1–5.

[63] C. Petus, G. Chust, F. Gohin, D. Doxaran, J.-M. Froidefond, and Y. Sagarminaga, "Estimating turbidity and total suspended matter in the Adour River plume (South Bay of Biscay) using MODIS 250-m imagery," *Continental Shelf Res.*, vol. 30, no. 5, pp. 379–392, 2010.

[64] M. Potes, M. J. Costa, and R. Salgado, "Satellite remote sensing of water turbidity in Alqueva reservoir and implications on lake modelling," *Hydrol. Earth Syst. Sci.*, vol. 16, no. 6, pp. 1623–1633, 2012.

[65] R. Nehorai *et al.*, "Satellite observations of turbidity in the Dead Sea," *J. Geophys. Res., Oceans*, vol. 118, no. 6, pp. 3146–3160, 2013.
[66] J.-K. Choi, Y. J. Park, B. R. Lee, J. Eom, J.-E. Moon, and J.-H. Ryu, "Application of the geostationary ocean color imager (GOCI) to mapping the temporal dynamics of coastal water turbidity," *Remote Sens. Environ.*, vol. 146, pp. 24–35, Apr. 2014.
[67] S. Chen, L. Han, X. Chen, D. Li, L. Sun, and Y. Li, "Estimating wide range total suspended solids concentrations from MODIS 250-m imageries: An improved method," *ISPRS J. Photogram. Remote Sens.*, vol. 99, pp. 58–69, Jan. 2015.
[68] E. Robert *et al.*, "Monitoring water turbidity and surface suspended sediment concentration of the bagre reservoir (Burkina Faso) using MODIS and field reflectance data," *Int. J. Appl. Earth Observ. Geoinf.*, vol. 52, pp. 243–251, Oct. 2016.
[69] F. Braga *et al.*, "Mapping turbidity patterns in the Po river prodelta using multi-temporal Landsat 8 imagery," *Estuarine, Coastal Shelf Sci.*, vol. 198, pp. 555–567, Nov. 2017.
[70] L. CarlosGonzález-Márquez, F. M. Torres-Bejarano, A. C. Torregroza-Espinosa, I. R. Hansen-Rodríguez, and H. B. Rodríguez-Gallegos, "Use of LANDSAT 8 images for depth and water quality assessment of El Guájaro reservoir, Colombia," *J. South Amer. Earth Sci.*, vol. 82, pp. 231–238, Mar. 2018.
[71] R. Ahmed, M. Sahana, and H. Sajjad, "Preparing turbidity and aquatic vegetation inventory for waterlogged wetlands in Lower Barpani sub-watersheds (Assam), India using geospatial technology," *Egyptian J. Remote Sens. Space Sci.*, vol. 20, pp. 243–249, Dec. 2017.
[72] S. Constantin, Ş. Constantinescu, and D. Doxaran, "Long-term analysis of turbidity patterns in Danube Delta coastal area based on MODIS satellite data," *J. Marine Syst.*, vol. 170, pp. 10–21, Jun. 2017.
[73] K. Li, G. Cheng, S. Bu, and X. You, "Rotation-insensitive and context-augmented object detection in remote sensing images," *IEEE Trans. Geosci. Remote Sens.*, vol. 56, no. 4, pp. 2337–2348, Apr. 2018.
[74] T. Tian, C. Li, J. Xu, and J. Ma, "Urban area detection in very high resolution remote sensing images using deep convolutional neural networks," *Sensors*, vol. 18, no. 3, p. 904, 2018.
[75] H. G. Ng, M. Z. MatJafri, K. Abdullah, and A. N. Alias, "Comparison of turbidity measurement by MODIS and AVHRR images," in *Proc. 5th Int. Conf. Comput. Graph., Imag. Visualisation*, Aug. 2008, pp. 398–403.
[76] *Turbidity in Source Water. EPA Guidance Manual, Turbidity Provisions*, U. S. E. P. A. EPA, Washington, DC, USA, 1999.
[77] A. Krizhevsky, I. Sutskever, and G. E. Hinton, "ImageNet classification with deep convolutional neural networks," in *Proc. Int. Conf. Neural Inf. Process. Syst.*, 2012, pp. 1097–1105.
[78] A. Graves, *Long Short-Term Memory*. Berlin, Germany: Springer, 2012.

YEQI LIU received the B.S. degree in communication engineering from China Agricultural University, Beijing, China, in 2017, where he is currently pursuing the M.S. degree in computer science and engineering from the College of Information and Electrical Engineering. His research interests include computer vision and neural networks.

YINGYI CHEN received the Ph.D. degree in agricultural information technology research from China Agricultural University, Beijing, China, in 2008. He is currently an Associate Professor of computer science and technology and the Deputy Director of the Department of Computer Engineering, College of Information and Electrical Engineering, China Agricultural University. He has published over 30 technical articles and taught 11 different courses related to computer science and technology and its application. Three of his master's students received the Graduate National Scholarship (2014, 2015, and 2016). He was involved in the research domains of agricultural information acquisition, information processing, big data analytics, and artificial intelligence.

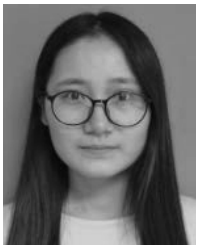

XIAOMIN FANG received the B.S. degree in Internet of Things from Jiangnan University, Wuxi, China, in 2017. She is currently pursuing the M.S. degree in computer science and engineering from the College of Information and Electrical Engineering, China Agricultural University, Beijing, China. Her research interests include machine learning and water quality prediction.